SANDIA REPORT

SAND93–0688 • UC–940
Unlimited Release
Printed January 1994

Observations of Quenching of Downward-Facing Surfaces

T. Y. Chu, B. L. Bainbridge, J. H. Bentz, R. B. Simpson

Prepared by
Sandia National Laboratories
Albuquerque, New Mexico 87185 and Livermore, California 94550
for the United States Department of Energy
under Contract DE-AC04-94AL85000

SF2900Q(8-81)

Issued by Sandia National Laboratories, operated for the United States Department of Energy by Sandia Corporation.

Printed in the United States of America. This report has been reproduced directly from the best available copy.

Available to DOE and DOE contractors from
Office of Scientific and Technical Information
PO Box 62
Oak Ridge, TN 37831

Prices available from (615) 576-8401, FTS 626-8401

Available to the public from
National Technical Information Service
US Department of Commerce
5285 Port Royal Rd
Springfield, VA 22161

NTIS price codes
Printed copy: A03
Microfiche copy: A01

SAND93-0688
Unlimited Release
Printed January 1994

Distribution
Category UC-940

Observations of Quenching of Downward-Facing Surfaces

T.Y. Chu, B.L. Bainbridge, J.H. Bentz, and R.B. Simpson

Sandia National Laboratories
Albuquerque, New Mexico

ABSTRACT

This report documents results of a series of scoping experiments on boiling from downward-facing surfaces in support of the Sandia New Production Reactor, Vessel-Pool Boiling Heat Transfer task. Quenching experiments have been performed to examine the boiling processes from downward-facing surfaces using two 61-centimeter diameter test masses, one with a flat test surface and one with a curved test surface having a radius of curvature of 335 cm, matching that of the Cylindrical Boiling facility test vessel.

Boiling curves were obtained for both test surfaces facing horizontally downward. The critical heat flux was found to be essentially the same, having an average value of approximately 0.5 MW/m^2. This value is substantially higher than current estimates of the heat dissipation rates required for in-vessel retention of core debris in the Heavy Water New Production Reactor as well as some of the advanced light water reactors under design. The nucleate boiling process was found to be cyclic with four relatively distinct phases: direct liquid/solid contact, nucleation and growth of bubbles, coalescence, and ejection.

TABLE OF CONTENTS

FIGURES

1.0 INTRODUCTION

The design of the Heavy Water New Production Reactor (HWR NPR) incorporates a flooded reactor cavity as an accident management feature to prevent melt-through of the reactor vessel in the event of a core meltdown accident. It is expected that boiling heat transfer on the outer surface of the bottom head will remove the decay heat from the molten core. The NPR Program at Sandia National Laboratories, sponsored by the Department of Energy, is undertaking a large-scale experimental evaluation of the flooded cavity design under the Vessel-Pool Boiling Heat Transfer (VPBHT) task. The task is designed to provide the necessary data to establish the safety margin of the proposed design. The boiling process on the bottom head in the flooded cavity design can be described as boiling on a large downward-facing curved surface. Although there exist a number of experimental studies of boiling on downward-facing surfaces, typical dimensions of the boiling surfaces are only on the order of a few centimeters (Chu, et al., 1992a, 1992b). Scaling of these results to the HWR NPR application is not possible.

One subtask of the VPBHT task is a series of subscale development tests to identify the key phenomena of boiling from downward-facing surfaces. The experiments are designed to provide insights into the phenomenology of downward-facing boiling. The scale of the experiments is between that of full-scale and typical bench-scale experiments, but it is by far the largest experiment of boiling from downward-facing surfaces.

2.0 EXPERIMENTS

A series of intermediate-scale quenching experiments was performed to examine the boiling processes from downward-facing axisymmetric surfaces. It is hoped that the experience gained from these experiments will aid in the interpretation of the large-scale experiment to be performed in Sandia's Cylindrical Boiling (CYBL) facility, and help in modelling the boiling processes.

Two test masses made of 6061 aluminum were used. They were made from 61 cm (24 in.) diameter stock approximately 10 cm (4 in.) thick. The first mass was a simple upright cylinder with a flat bottom (Figure 1). The second mass was similar to the first, except that the bottom surface had a radius of curvature of 335 cm (132 in.) (Figure 1), matching the crown radius of the CYBL test vessel. The experimental masses were heated to an elevated temperature between 160°C and 330°C, and then plunged into a pool of water at saturation. The vertical surfaces and the top of the experimental masses were insulated to limit the boiling to only the downward-facing surfaces. Figure 2 shows how the masses were machined such that the Visilox^R silicone rubber insulating layers were set into the surface so that the test surface extended all the way to the edge of the test mass, and the two-phase flow across the test surface would not encounter an abrupt obstruction.

The test masses were instrumented with seven pairs of near-surface thermocouples. Each pair consisted of a thermocouple at a depth of 0.64 cm (0.25 in) and one at a depth at 1.27 cm (0.5 in). The near-surface thermocouples were located at radii 1.27 cm (0.5 in) to 27.94 cm (11 in) as shown in Figures 1 and 2. The thermocouples used were type K, 1.6 mm (1/16 in.) diameter stainless steel sheathed thermocouples with grounded junctions. These thermocouples were chosen because they will be used in the large-scale experiments. For ease of installation, the near-surface thermocouples were installed from the water side. Observations during the quenching experiments indicated that the presence of the thermocouples did not cause significant disturbance to the overall characteristics of the boiling process. There were also three thermocouples 1.27 cm (0.5 in) below the top surface of the test mass for interior temperature measurements.

The test surface was machined to a No. 32 finish and then brushed with a fine steel brush. Figure 3 shows the typical surface texture as machined and after brushing. To ensure identical starting conditions for each experiment, the surface finish was renewed before each experiment by brushing. Each mass was supported from above by a rod screwed into the top. The other end of the rod was connected to an air cylinder that allowed for vertical motion.

The sample was first heated by six two-kilowatt cartridge heaters to the desired initial temperature. After a brief waiting period, when the temperatures were observed to equilibrate, the experiment was initiated by extending the air cylinder and plunging the mass into a test vessel filled with water. The test vessel was a Lexan^R box, 91 cm on each side. The box was filled with de-ionized water to a depth of 60 cm, and the test surface was immersed approximately 15 cm below the water surface. Two auxiliary heaters were used to keep the water at saturation. The quenching process was videotaped through windows in the bottom and the side of the Lexan^R tank.

A Hewlett Packard model 3852, 5½ digit integrating analog-to-digital converter was used for data acquisition. The sampling interval was slightly under 0.5 seconds.

2.1 Experimental Observations

As a test mass is quenched from an elevated temperature it goes through film boiling, transition boiling, critical heat flux, and finally nucleate boiling.

The liquid/vapor interface during film boiling appears to be relatively stable. The surface can best be described as a visually smooth film with superimposed small amplitude waves, as shown in Figure 4. The initiation of transition boiling from film boiling is signaled by the appearance of groups of bulges in the vapor film moving around the edge of the test surface. Eventually, the number and locations of bulges around the edge increases, and the bulges move inward to extend across the entire surface.

Transition boiling is characterized by intermittent direct liquid/solid contacts and a liquid/vapor interface with growing and receding bulges, as shown in Figures 4 and 5. Over time, the interface appears to have a rather uniform appearance. The typical dimension of bulges is of the order of 1 cm. The intermittent solid/liquid contacts appear as swirling clouds moving around the surface. The cloudy appearance is probably associated with the rapid vaporization at the contact sites.

As the mass cools further, the critical heat flux (CHF) is reached. The CHF regime is characterized by cyclic explosive vaporization. Shown in Figure 6 is one such cycle. The cycle starts with a surface covered completely with a vapor film. A small indentation appears in the film probably leading to direct liquid/solid contact. This initial disturbance results in an ever expanding circular region of intense vaporization. As the circular region expands, the vapor film outside of the circle is pushed beyond the edge and released into the bulk liquid. As shown in the side-view in Figure 7, the vapor mass extends as much as five centimeters away from the surface. The periods of this cyclic event for the flat specimen and the curved specimen are 0.29 and 0.27 seconds, respectively. In time, the explosions become less intense and less far-reaching. While the vapor film thickness still undulates, the amplitude becomes much less. Subsequently, the mass enters the nucleate boiling regime.

Visual observation indicates that nucleate boiling from downward-facing surfaces is a cyclic process. Starting with direct liquid/solid contact, bubbles nucleate at various sites. These bubbles grow and coalesce into larger bubbles (Figures 4 and 8). For the flat surface at high heat fluxes ($q > 0.1$ MW/m^2), the coalescence phase ends with nearly the entire surface covered with one single vapor mass.

At high heat fluxes, the ejection phase is vigorous and chaotic. The large single vapor mass may break into several pieces and slide off the surface in several directions or shed away as a single entity. However, over time, the process appears to be quite rhythmic and the directions in which the vapor masses leave appear to be random. At high heat fluxes, nucleation takes place immediately at the freshly exposed surfaces left by the shedding fragments of the large vapor mass. Therefore, the ejection phase of the first cycle and the growth phase of the second cycle actually overlap in time; the surface is partly covered by large retreating vapor masses of the first generation and the new bubbles of the second generation nucleating and growing in between the retreating large vapor masses (Figure 9). At intermediate heat fluxes (0.03 M/m^2 $< q <$ 0.1 MW/m^2) bubbles do not always grow to cover the entire surface before the ejection phase (Figure 10). For low heat fluxes ($q <$ 0.03 MW/m^2), the nucleation sites become far apart and bubble coalescence becomes increasingly local in scale. Eventually, at lower heat fluxes, the surface is covered with a few growing bubbles lumbering toward the edge of the surface with a significant portion of the surface in direct contact with the bulk liquid. For the curved surface, the cyclic process still applies. However, as a result of the geometry the shedding of the vapor masses from the surface is more regular, always taking a more or less radial direction, especially at lower heat fluxes. It is also interesting to note, for the curved surface at low heat fluxes, the bubbles take a crescent shape as they move toward the edge of the surface, as shown in Figure 10.

The thermocouple data are processed with an inverse conduction code SODDIT (Blackwell et al., 1987) to obtain boiling curves. SODDIT is a finite difference code that can be used to solve one and quasi-two-dimensional direct and inverse heat conduction problems. When solving inverse problems, the unknown surface heat flux is calculated by minimization of the squared error between the temperatures measured at specified locations and the corresponding computed temperatures. In addition, more than one future time can be used in the heat flux calculation to reduce the effect of measurement error and noise.

During preliminary experiments, it was discovered that while the cooling rates over the test surface were reasonably uniform during film boiling; the rates started to diverge considerably as transition boiling approached. Transition boiling occurred first near the edge of the test surface and moved inward. Therefore, the heat transfer within the mass became multi-dimensional. As a result, different locations on the surface underwent critical heat flux at different times, making it highly inaccurate to use the SODDIT code to calculate the surface flux. However, if the initial temperature were in the range of transition boiling, the temperature response over the surface became nearly uniform. This is probably related to the nearly uniform appearance of the surface during transition boiling (Figure 5). Therefore, two sets of experiments were performed. High temperature quench from 330°C was used to obtain the film boiling to transition boiling portion of the boiling curve, and low temperature quench from 160°C to 170°C was used to obtain the transition boiling to nucleate boiling portion of the curve.

A composite boiling curve for the flat specimen from three low temperature quench experiments and one high temperature quench experiment is shown in Figure 11. The critical heat flux is found to be between 0.4-0.6 MW/m^2; the corresponding superheat is approximately 30°C. The spread of the data represents an experimental uncertainty of approximately $\pm$ 20%. This critical heat flux is higher than those reported for previous experiments using 15-m test masses (Chu et al., 1992b). We feel that the previous results are in error because data rates were too low, and the quenching curve failed to resolve the high cooling rates associated with the critical heat flux. The present CHF values are also higher than those obtained by Guo and El-Genk (1991) quenching a 50mm copper disk. We believe the Guo and El-Genk CHF value is low because of the effect of the insulation rim around their quenching specimen. As shown in Ishigai et al. (1961) experiments, the CHF value decreases by almost a factor of two with the size of the insulating rim around the Guo and El-Genk test specimen.

The 10°C superheat corresponding 0.1 MW/m^2 is in good agreement with previous quenching experiments (Chu et al., 1992b) as well as the results of Nishikawa et al. (1984) and Guo and El-Genk (1991). A boiling curve is also calculated for the curved specimen (Figure 12). The critical heat flux is essentially the same as that for the flat surface. The nucleate boiling portion of the curve is slightly below that for the flat surface. This is consistent with previously observed trends of the effects (Nishikawa, et al., 1984, Guo and El-Genk 1991) of surface inclination.

It is interesting to note that there appears to be a rather distinct change of slope of the boiling curve near 0.1 MW/m^2. This transition is analogous to the transition from the isolated bubble regime to that of slugs and columns for upward-facing surfaces, as first pointed out by Lienhard (1985). As described earlier, for heat flux less than 0.1 MW/m^2, the bubbles do not always grow large enough to coalesce into a large vapor mass to cover the entire surface before the ejection phase. But for higher heat fluxes, the ejection phase is always associated with a surface-size vapor mass. There are also changes in the rhythmic/cyclic behavior of the boiling process associated with the transition. The general trend is for the cycle period to increase (as well as the nucleation site density to decrease) with decreasing heat flux. Between critical heat flux and 0.1 MW/m^2, the cycle time increased by about 17%. Whereas, between 0.1 MW/m^2 and 0.05 MW/m^2, the cycle time increased by more than 30%.

3.0 CONCLUDING REMARKS

Quenching experiments have been performed to examine the boiling processes from downward-facing surfaces using two 61-centimeter diameter test masses, one with a flat test surface and one with a curved test surface having a radius of curvature of 335 cm. Boiling curves were obtained for both test surfaces facing horizontally downward. The critical heat flux was found to be essentially the same, having an average value of approximately 0.5 MW/m^2. This value, while smaller than the accepted value of CHF for upward-facing surfaces (typically 1-1.3 MW/m^2), is larger than those obtained from correlations derived from smaller scale experiments (Guo and El-Genk, 1991; Vishnev et al., 1976). The critical heat flux is significantly higher than the estimated heat fluxes required for in-vessel retention for the HWR NPR (Jedruch, 1992) and for light water reactors (Henry, et al., 1993); those values are 0.16 MW/m^2 and 0.20 MW/m^2, respectively.

The liquid/vapor interface during film boiling appears to be relatively stable. The traveling bubble pattern obtained by Bui and Dhir (1985) was not observed. The surface can best be described as a visually smooth film with superimposed small amplitude waves.

Transition boiling is characterized by intermittent direct liquid/solid contacts and a liquid/vapor interface with growing and receding bulges. Over time, the interface appears to have a rather uniform appearance. The typical dimension of bulges is of the order of 1 cm.

The critical heat flux regime is characterized by cyclic explosive vaporization with circular expansion patterns. The periods of this cyclic event for the flat specimen and the curved specimen are 0.29 and 0.27 seconds, respectively.

The nucleate boiling process is found to be cyclic with four relatively distinct phases: direct liquid/solid contact, nucleation and growth of bubbles, coalescence, and ejection. The general trend is for the cycle time to increase with decreasing heat flux.

Traditionally, experiments aimed at investigating basic mechanisms of boiling and theoretical treatments of boiling have concentrated on upward-facing flat surfaces. Other geometries have been treated as extensions of upward-facing surfaces. However, the current experiments reveal rather unique flow patterns compared to those observed from upward-facing surfaces. While there are similarities in the initial nucleation and growth of bubbles, there appear to be substantial differences in the mechanisms of late-phase growth, coalescence and detachment of vapor masses in the nucleate boiling regime, and in the appearance of near surface two-phase flow, approaching CHF. None of the key mechanisms of the current hydrodynamic stability based theory of CHF are operational in downward-facing boiling. However, both boiling processes generate the characteristic boiling curve. It is appropriate to recall a recent lecture by Bergles (1992): "nucleate boiling still defies accurate prediction [and]... there is a lack of agreement on the mechanism of critical heat flux." The present observations, although qualitative and preliminary, suggest that perhaps by examining upward-facing and downward-facing boiling in parallel experiments, it would be possible to single out a common set of mechanisms that give rise to the boiling curve. These mechanisms can then be considered necessary and sufficient to build a mechanistic model of boiling.

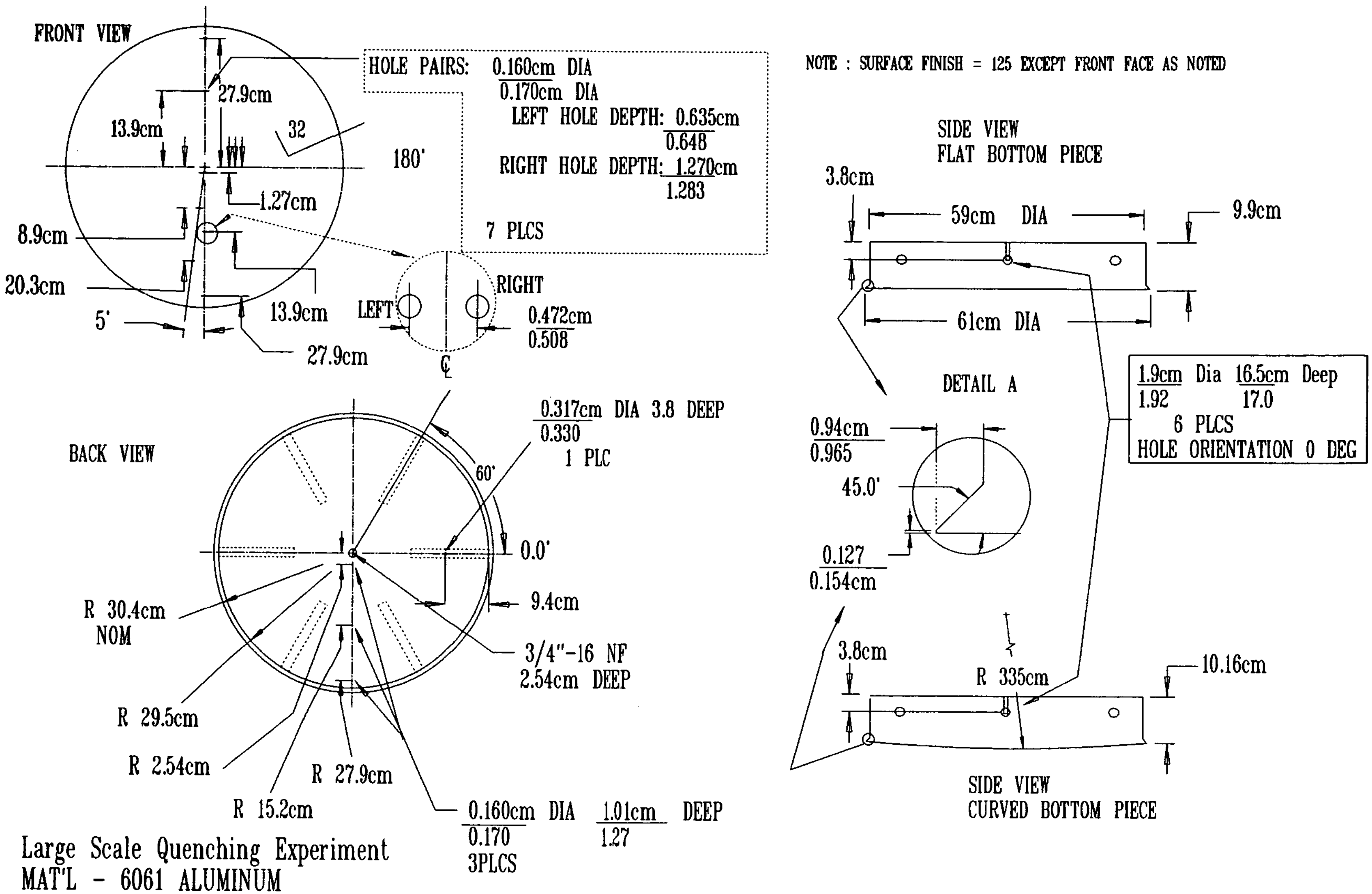

Figure 1. Design of Test Specimens

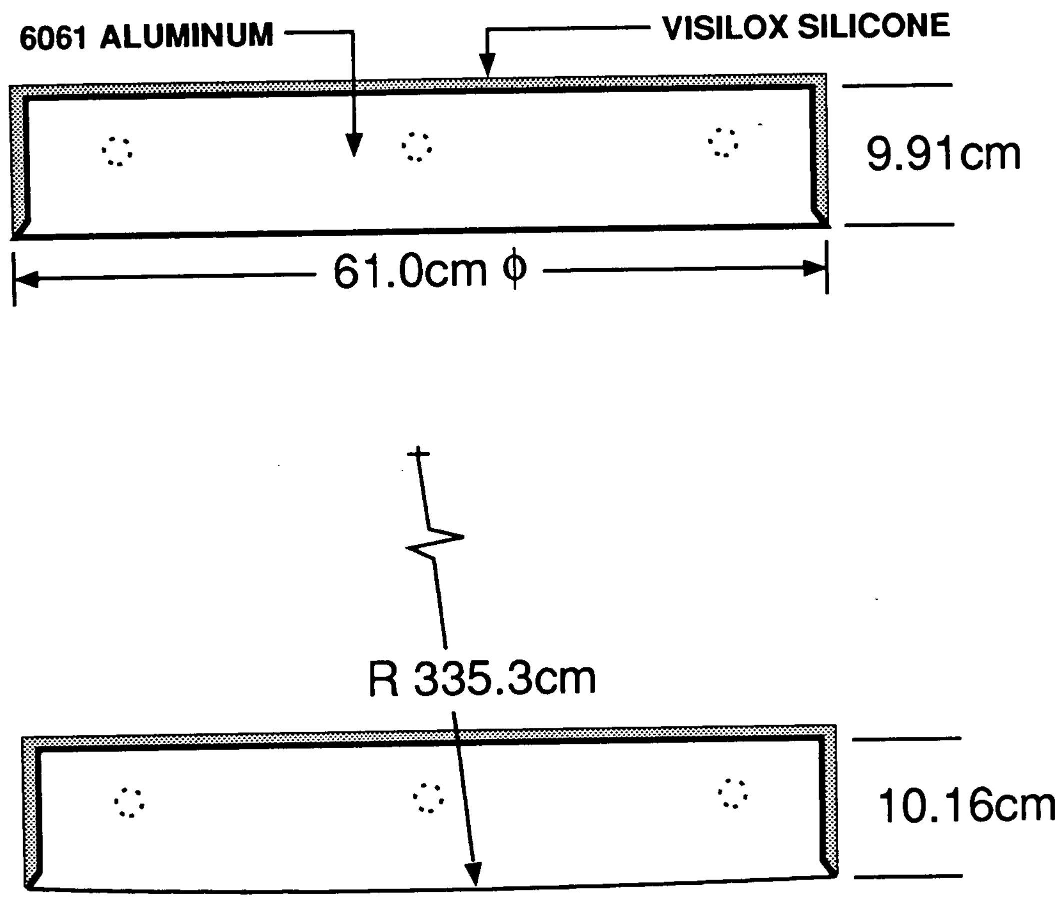

Figure 2. Design of Test Specimen Insulation

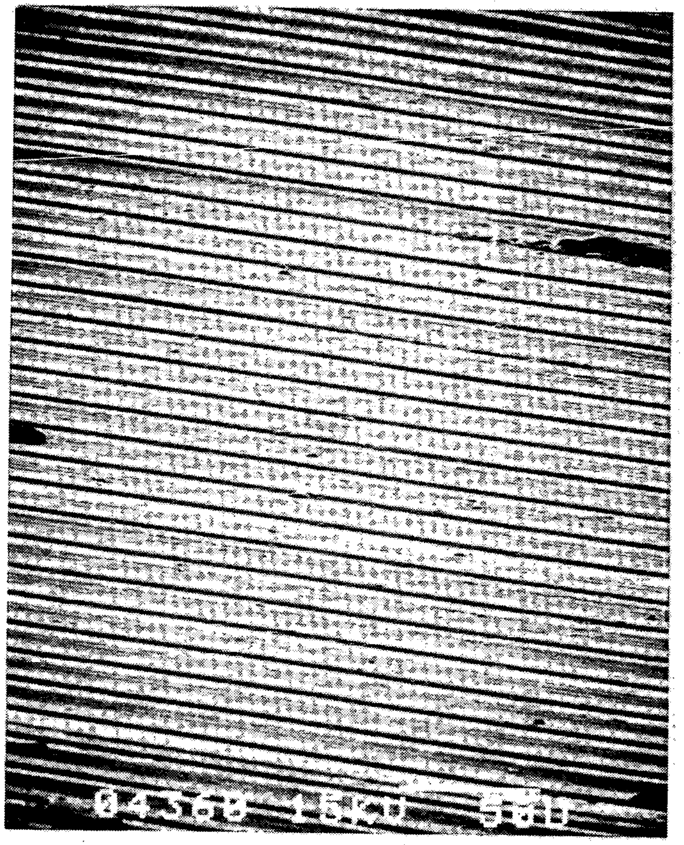

As Machined

After Brushing

Figure 3. Scanning Electron Micrograph of Test Surface, 400X and 70° Viewing Angle

Film Boiling

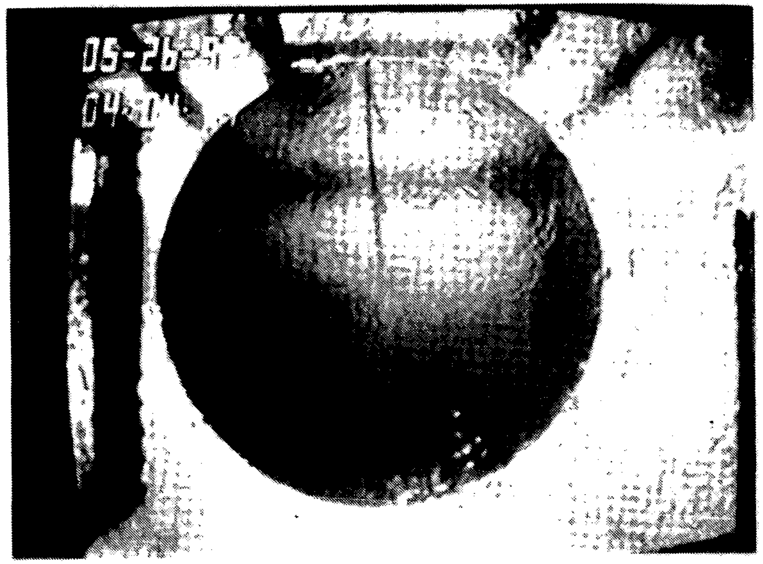

Film Boiling Instability

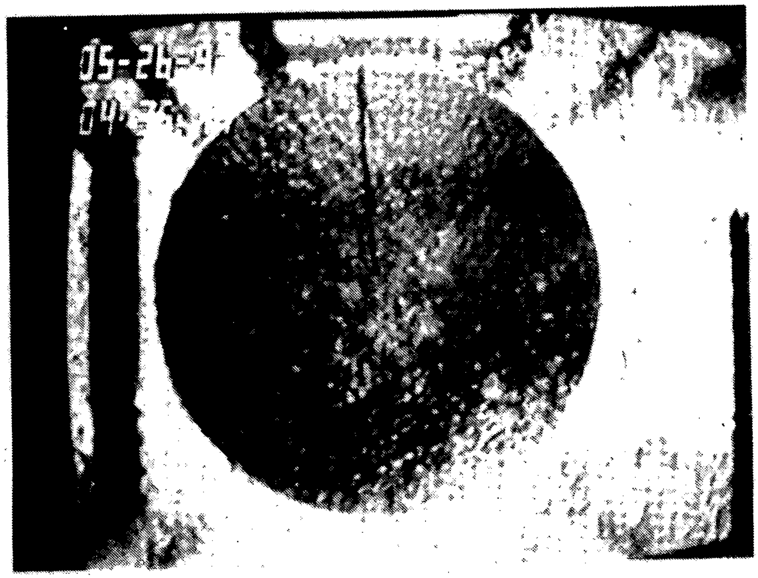

Transition Boiling

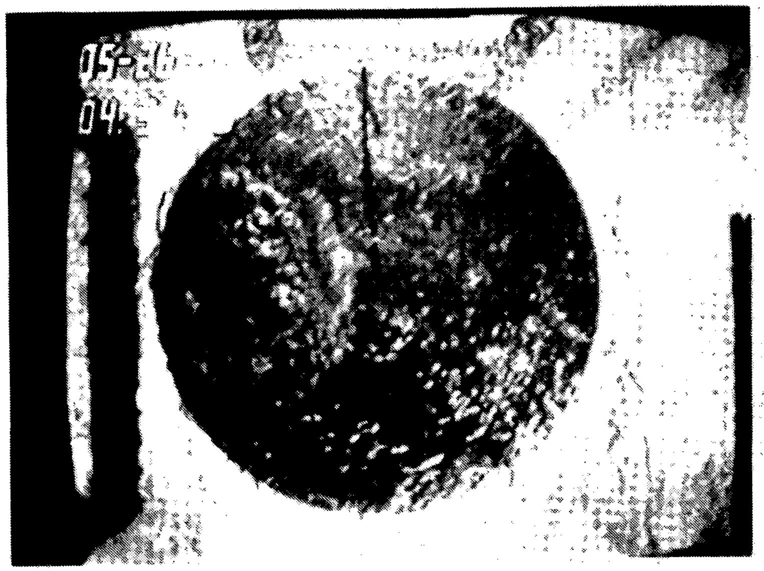

Nucleate Boiling (High Heat Flux)

Figure 4. Video Frames of the General Appearance of Liquid/Vapor Interface for Different Boiling Regimes.

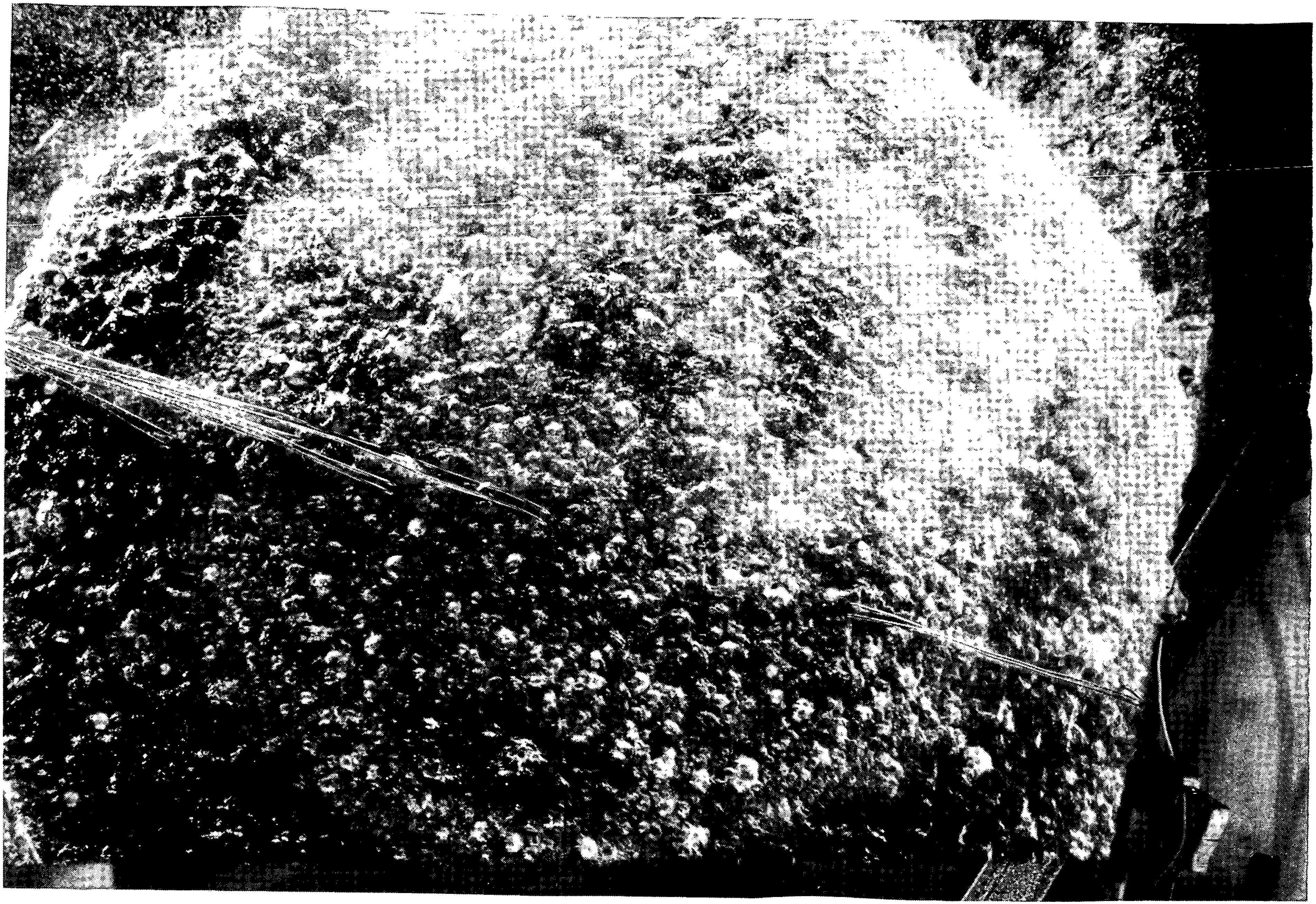

Figure 5. Photograph of the Liquid/Vapor Interface in Transition Boiling

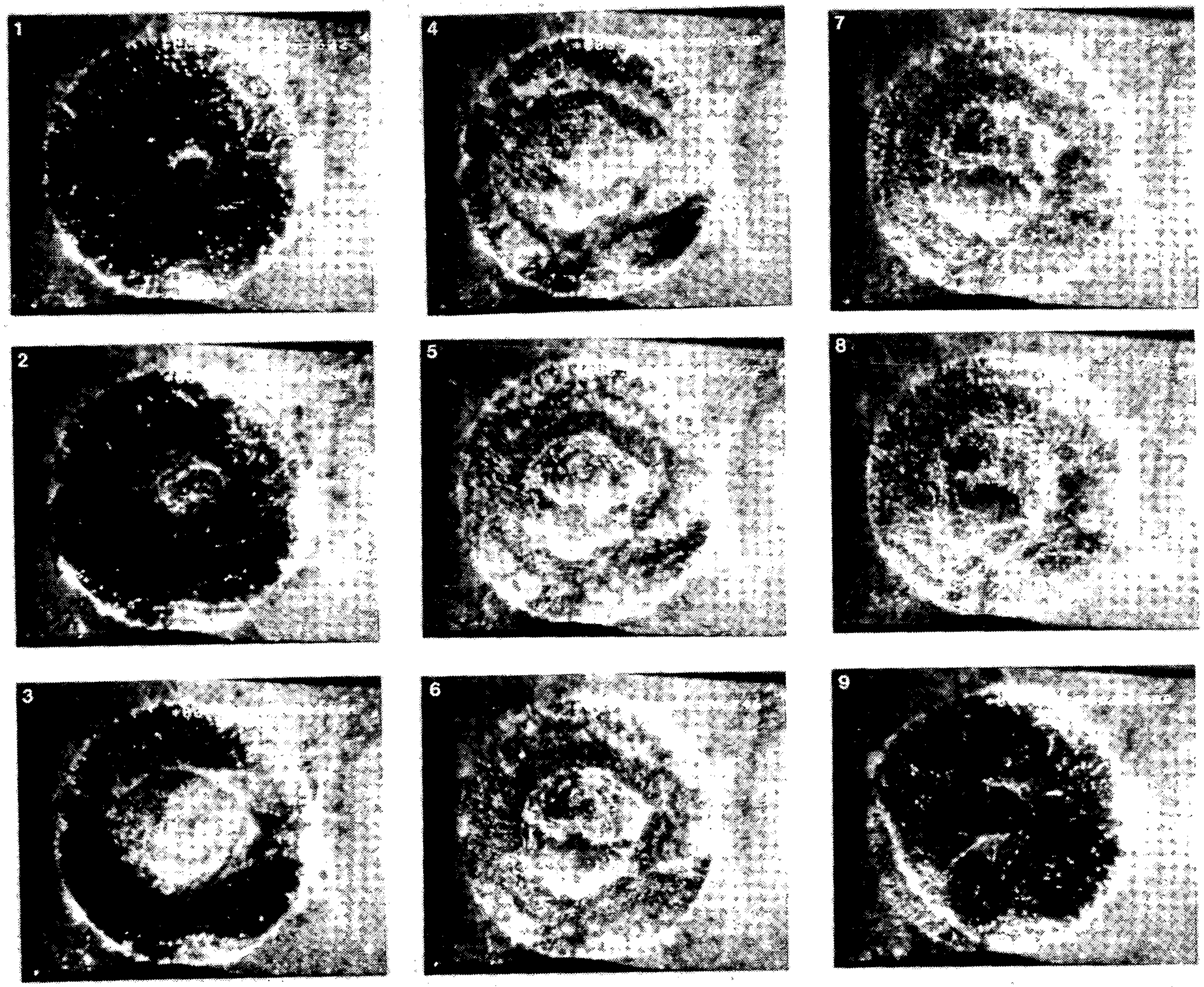

CRITICAL HEAT FLUX (Run ALFLATAH)

Figure 6. Video Frames of a Cycle of Explosive Vapor Formation at CHF, Bottom View

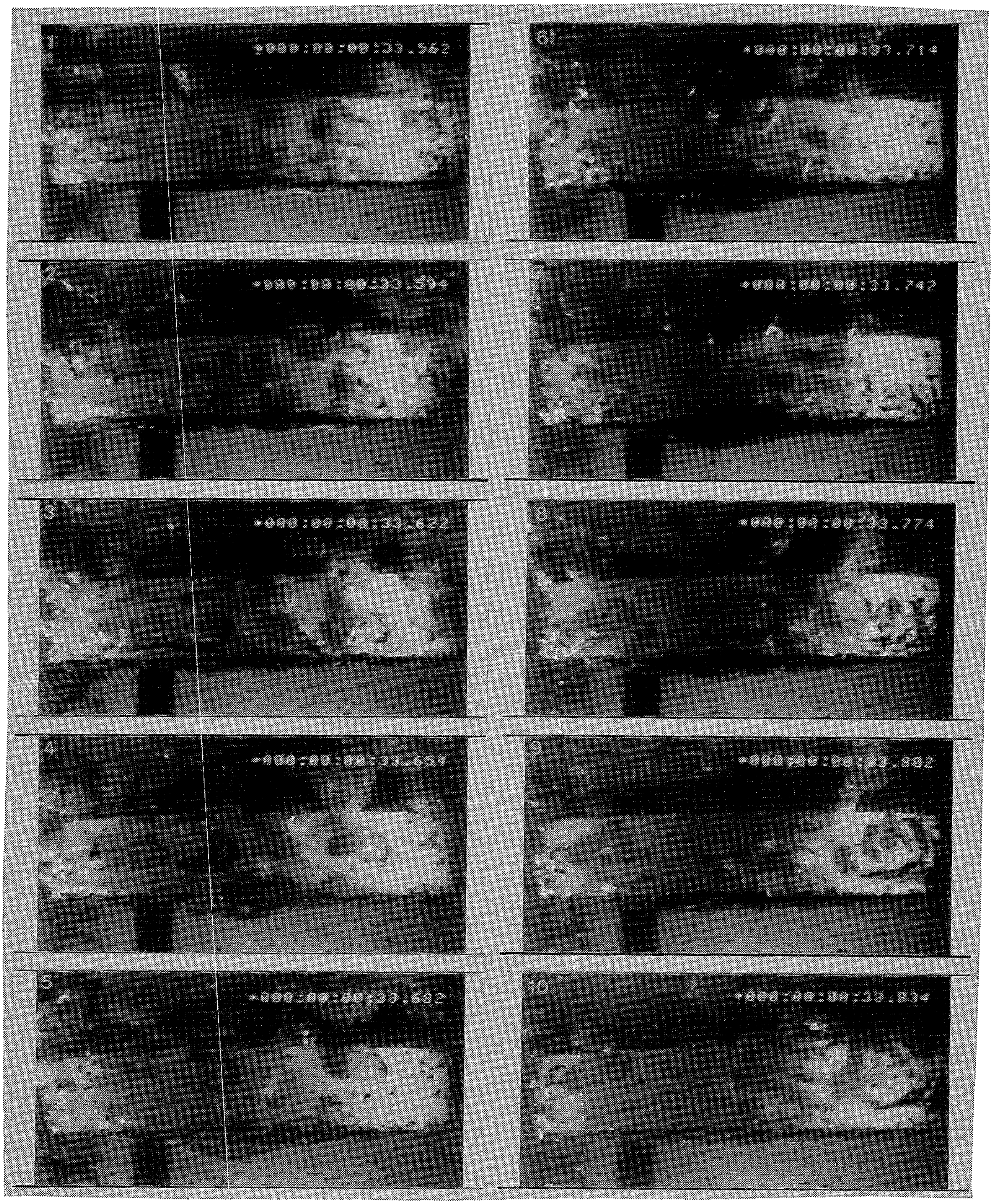

Figure 7. Video Frames of a Cycle of Explosive Vapor Formation at CHF, Side View

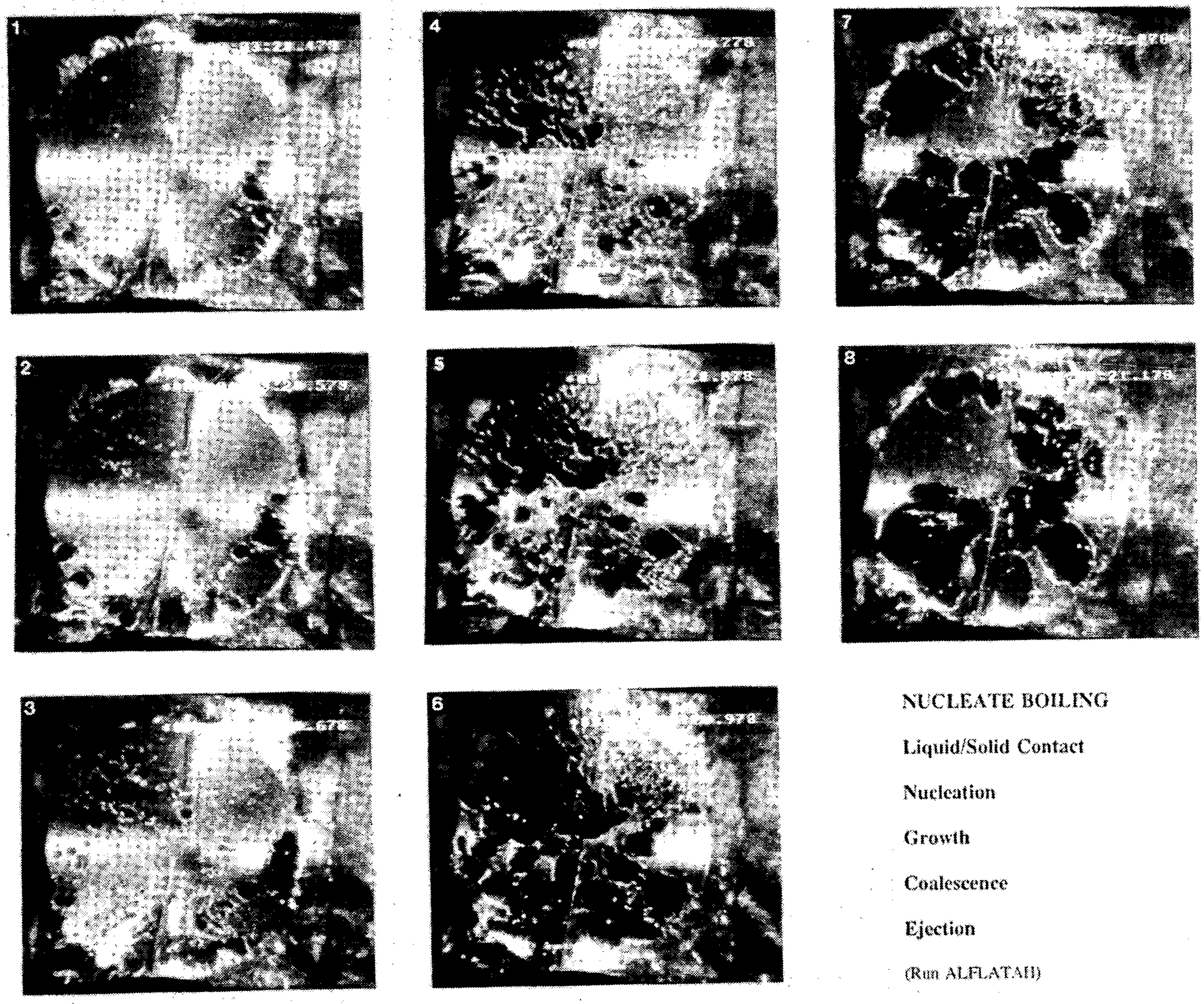

NUCLEATE BOILING

Liquid/Solid Contact

Nucleation

Growth

Coalescence

Ejection

(Run ALFLATAH)

Figure 8. Video Frames of Nucleate Boiling at Intermediate Heat Fluxes

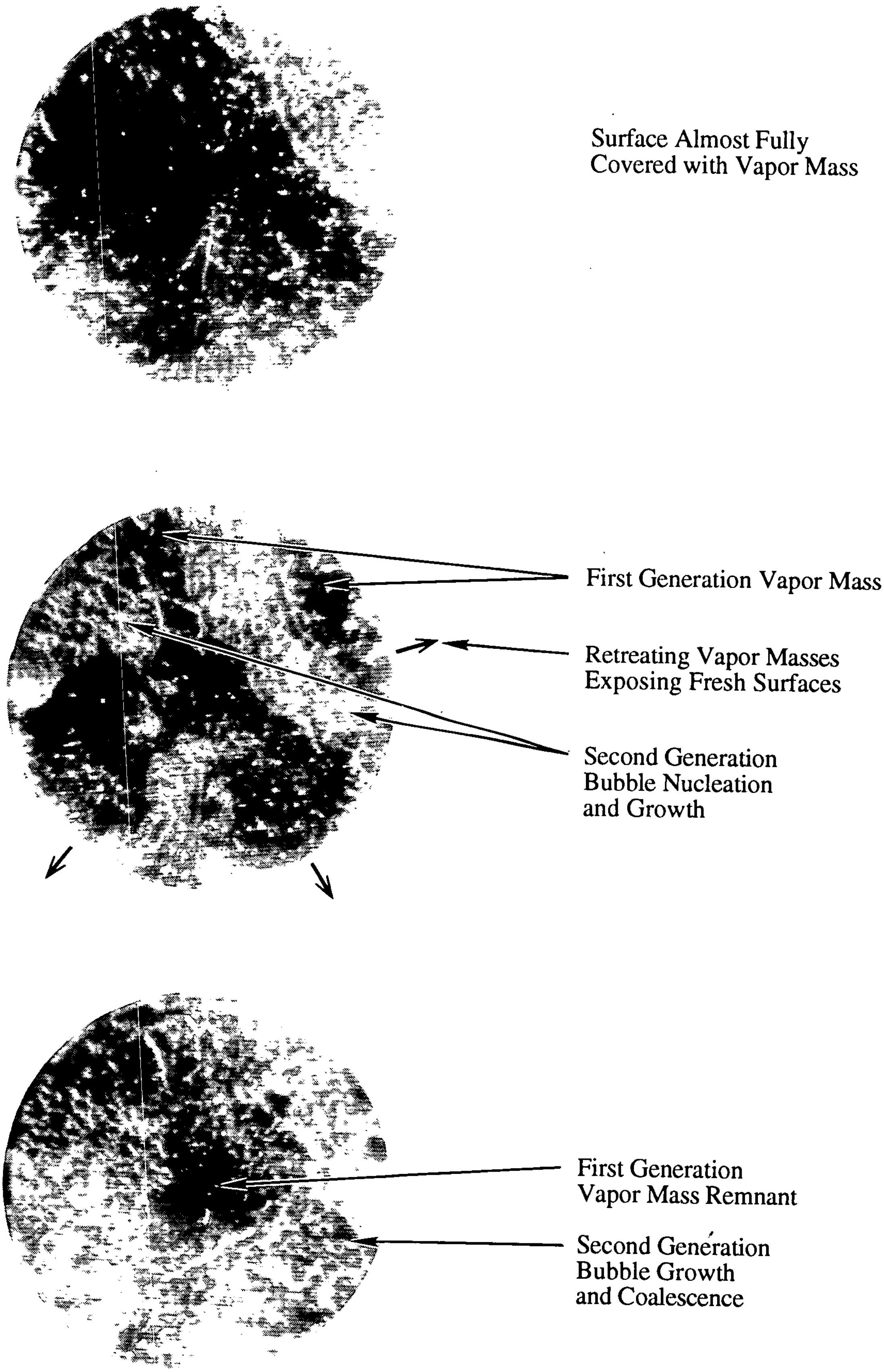

Figure 9. Video Frames of Nucleate Boiling at High Heat Fluxes

Figure 10. Video Frames of Nucleate Boiling at Low Heat Fluxes on the Curved Bottom Test Specimen

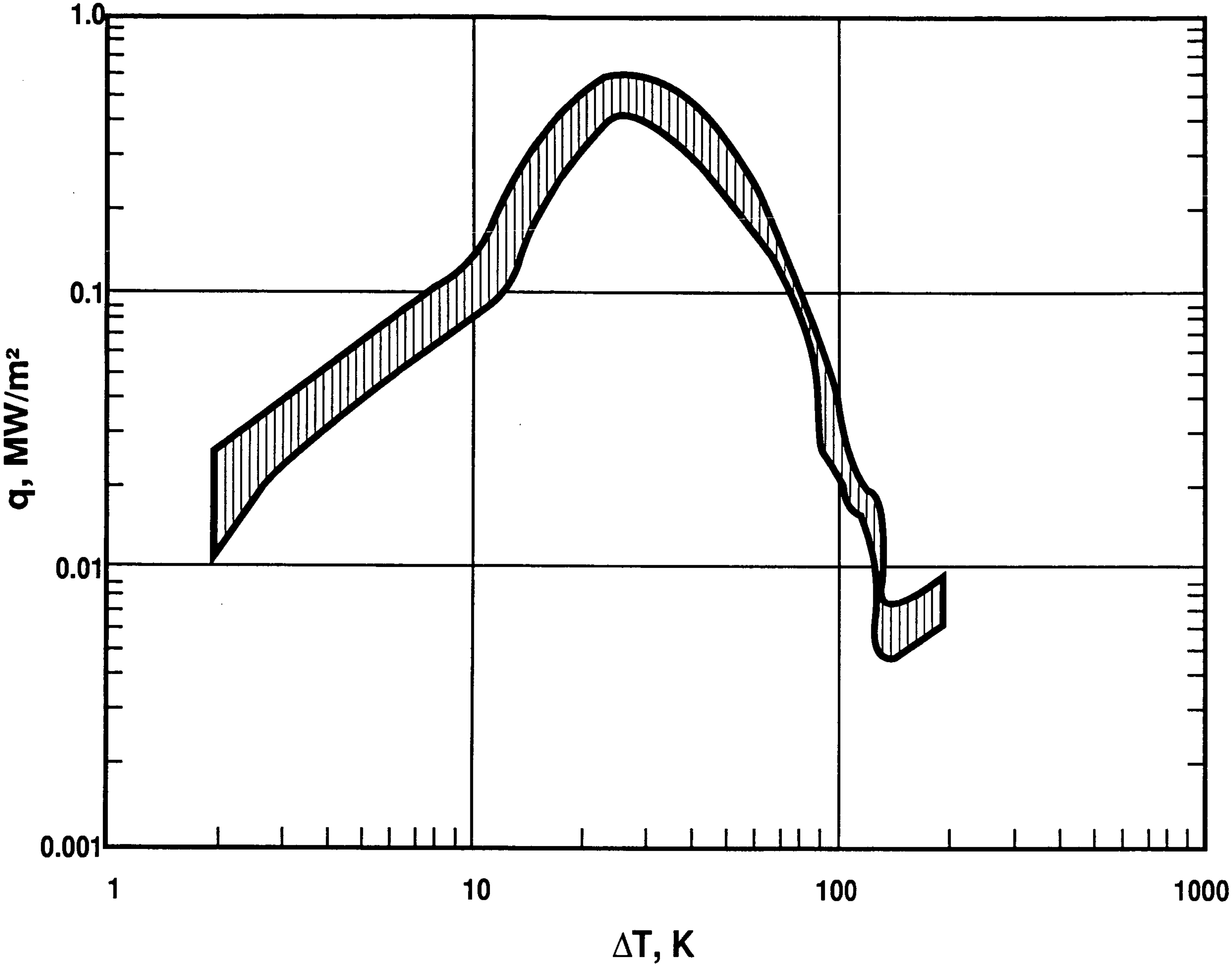

Figure 11. Boiling Curve from Flat Test Specimen

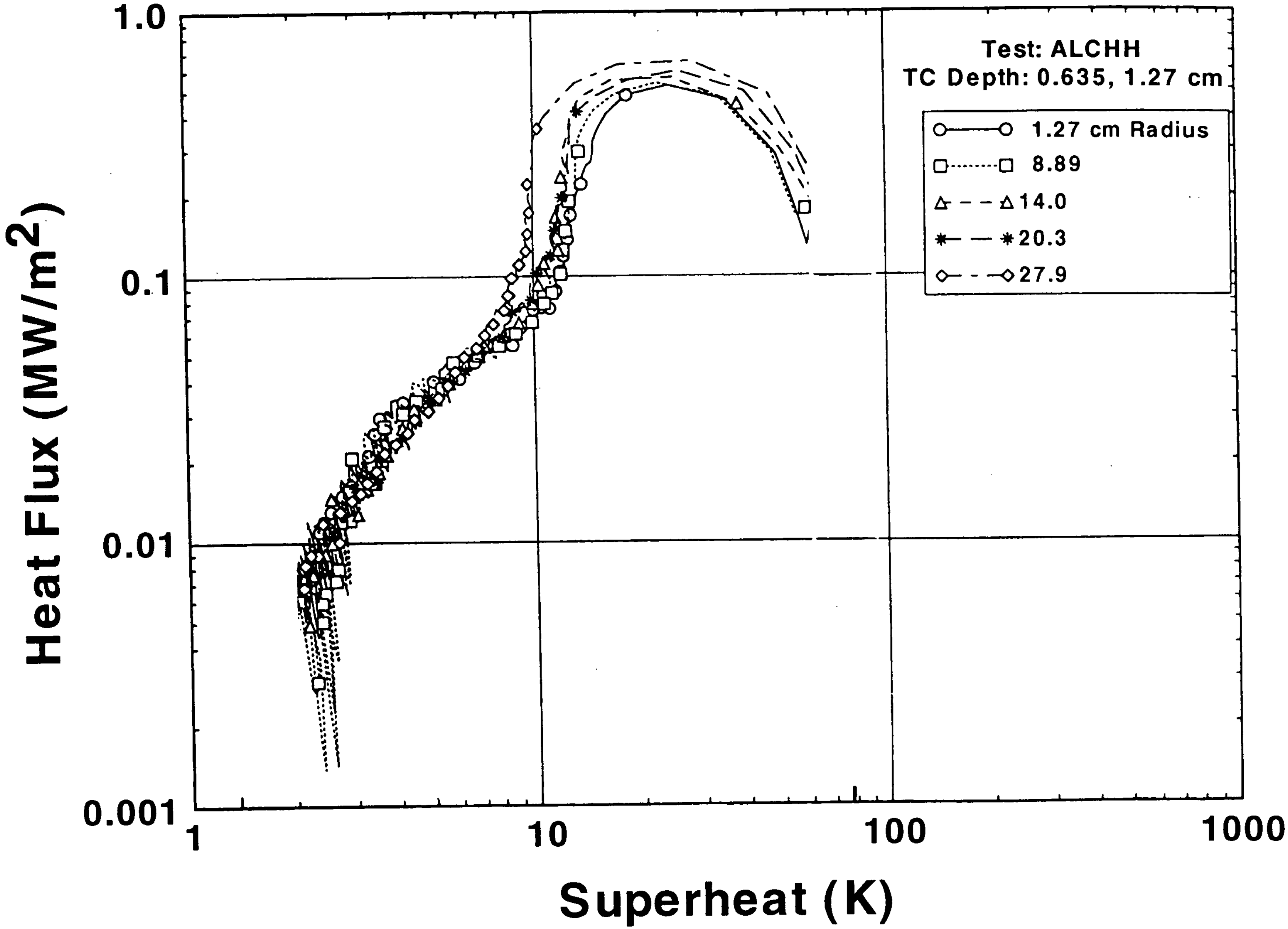

Figure 12. Boiling Curve from Curved Test Specimen

4.0 REFERENCES

Bergles, A. E., 1992, "What are the Real Mechanisms in Pool Boiling?" Pool and External Flow Boiling, Eds., V. K. Dhir and A. E. Bergles, ASME, New York, NY.

Blackwell, B. F., R. W. Douglass, and H. Wolf, 1987, A User's Manual for the Sandia One-Dimensional Direct and Inverse Thermal (SODDIT) Code, SAND85-2478, Sandia National Laboratories, Albuquerque, NM.

Bui, T. D., and V. K. Dhir, 1985, "Film Boiling Heat Transfer on an Isothermal Vertical Surface," J. Heat Trans., Vol. 107, pp. 764-771.

Chu, T. Y., R. C. Dykhuizen, and C. E. Hickox, 1992a, Scoping Studies of Boiling Phenomena Associated with the Flooded Cavity Design of the Heavy Water New Production Reactor, NPRW-SA92-2, Sandia National Laboratories, Albuquerque, NM.

Chu, T. Y., R. C. Dykhuizen, and C. E. Hickox and B. L. Bainbridge, 1992b, "Boiling from Downward Facing Surfaces with Applications to the Flooded Cavity Concept," ANS Proceedings, 1992 National Heat Transfer Conference, San Diego, CA, HTC-Vol.6, pp. 367-375.

Guo, Z., and M. S. El-Genk, 1991, "An Experimental Study of the Effect of Surface Orientation on Boiling Heat Transfer During Quenching," Proceedings ASME Winter Annual Meeting, Atlanta, GA, Dec. 2-5.

Henry, R. E., J. P. Burelbach, R. T. Hammersley, C. E. Henry and G. T. Klopp, 1993, "Cooling of Core Debris within the Reactor Vessel Lower Head," Nuclear Technology, Vol. 101, pp. 385-399.

Ishigai, S., K. Inoue, Z. Kiwaki, and T. Inai, 1961, "Boiling Heat Transfer from a Flat Surface Facing Downward," Proceedings of International Heat Transfer Conference, Boulder, Colorado, 1961, p. 224-229.

Jedruch, J., 1992, Post-Melt Heat Flux Estimate in 670 MWt NPR Lower RV Head, EBASCO Services Inc. Report, New York, NY.

Lienhard, J. H., 1985, "On the Two Regimes of Nucleate Boiling", J. Heat Trans., Vol. 107, pp. 262-264.

Nishikawa, K., Y. Fujita, S. Uchida, and H. Ohta, 1984, "Effect of Configuration on Nucleate Boiling Heat Transfer," Int. J. Heat Mass Transfer, Vol. 27, pp. 1559-1571.

Vishnev, I. P., I. A. Filatov, Y. A. G. Vinokur, V. V. Gorokhov, and V. V. Svalov, 1976, "Study of Heat Transfer in Boiling of Helium on Surfaces With Various Orientations," Heat Transfer - Soviet Research, Vol. 8, No. 4, pp. 194-108.

DISTRIBUTION

82 copies for UC-940

Additon, Steve
Tenera
7272 Wisconsin Ave.
Bethesda, MD 20814

Baker, L.
Argonne National Laboratories
9700 South Cass Avenue
Building 208
Argonne, IL 60439

Catton, Ivan
University of California Los Angeles
Nuclear Energy Laboratory
405 Hilgard Avenue
Los Angeles, CA 90024

Cheung, Fan-Bill
Professor of Mechan. Engineering
The Pennsylvania State University
208 Reber Building
University Park, PA 16802-1413

Cho, Dae H.
Argonne National Laboratory
RAS, Building 208
9700 South Cass Avenue
Argonne, IL 60439-4842

Chyu, Ming-C.
Professor
Dept. of Mechan. Engineering
Texas Tech University
Box 4289
Lubbock, TX 79409-1021

Corradini, Mike L.
University of Wisconsin
Department of Nuclear Energy
1500 Johnson Drive
Madison, WI 53706

Dhir, Vijak K.
Professor
School of Engineering
38-137E Engr IV
University of California
Los Angeles, CA 90024

El-Genk, Mohamed S.
Professor
Dept. of Chem. and Nuclear Eng.
The University of New Mexico
Albuquerque, NM 87131

Fauske & Associates, Inc. (4)
Attn: M. Epstein
H.K. Fauske
R.J. Hammersley
R. Henry
16W070 West 83rd Street
Burr Ridge, IL 60521

Franks, Sterling, III
LWR Safety & Technology
Branch, NE-451
U.S. Department of Energy
19901 Germantown Road
Germantown, MD 20874

Greene, George A.
Experimental Heat Transfer
and Fluid Dynamics Group
Department of Nuclear Energy
Building 820M
Brookhaven National Laboratory
Upton, NY 11973

Guppy, James
Experimental Heat Transfer
and Fluid Dynamics Group
Department of Nuclear Energy
Building 820M
Brookhaven National Laboratory
Upton, NY 11973

Haugh, J.
Electric Power Research Institute
3412 Hillview Avenue
P.O. Box 10412
Palo Alto, CA 94303

Jedruch, Jacek
Ebasco Services, Inc.
Two World Trade Center - 89th Floor
New York, NY 10048

Leaver, D.E.
Polestar
Four Main Street
Los Altos, CA 94022

Lienhard, J.H.
Professor
Dept. of Mechanical Eng.
University of Houston
Houston, TX 77204-4792

Massachusetts Institute of Technology (2)
Department of Nuclear Energy
Building 24
Attn: Mujid Kazimi
Neil Todreas
77 Massachusetts Avenue
Cambridge, MA 02139

Pasedag, Walter F.
U.S. Department of Energy
ALWR, NE-451
Washington, DC 20545

Podowski, Michael
Department of Nuclear Engineering
and Engineering Sciences
Rensselaer Polytechnic Institute
NES Building
Tibbits Avenue
Troy, NY 12180-3590

Scobel, James
Westinghouse Energy Center
Ms 3-09 East
Northern Pike & Haymaker Roads
Monroeville, PA 15146

Simon, Terrance W.
Professor
Dept. of Mechan. Eng.
University of Minnesota
125 Mech. Eng. Bldg.
111 Church St. S.E.
Minneapolis, MN 55455

Sorrell, Steven
U.S. Department of Energy
785 DOE Place
Mail Stop 1134
Idaho Falls, ID 83415

Theofanous, Theo G.
University of California
Department of Chemical and
Nuclear Engineering
Santa Barbara, CA 93106

U.S. Nuclear Regulatory Commission (3)
Office of Nuclear Regulatory Research
S. Basu, MS: NLN344
F. Eltawila, MS: NLN344
R.W. Wright, MS: NLN344
Washington, DC 20555

U.S. Nuclear Regulatory Commission
Office of Nuclear Regulatory Research
B.W. Sheron, MS: NLS007
Washington, DC 20555

SANDIA DISTRIBUTION:

MS0100	Document Processing for DOE-OSTI (10) (7613-2)
MS0619	Technical Publications (7151)
MS0736	N.R. Ortiz (6400)
MS0739	K.E. Washington (6429)
MS0741	A.K. Moonka (6471)
MS0741	S. Slezak (6471)
MS0743	K. Bergeron (6907)
MS0744	D.A. Powers (6404)
MS0744	W.A. von Riesemann (6403)
MS0827	C.E. Hickox (1511)
MS0835	R.C. Dykhuizen (1513)
MS0835	B.L. Bainbridge (1513)
MS0899	Technical Library (5) (7144)
MS1135	N.R. Keltner (2761)
MS1135	D.H. Schulze (2761)
MS1135	D.L. Shamblin (2761)
MS1137	M.D. Allen (6422)
MS1137	T.Y. Chu (15) (6422)
MS1139	J.H. Bentz (6423)
MS1139	A.W. Reed (6423)
MS1139	K. Reil (6423)
MS1139	R. Simpson (6423)
MS9211	Central Technical Files (8523)